A microelectrode array (MEA) integrated with clustering structures for investigating in vitro neurodynamics in confined interconnected sub-populations of neurons

L. Berdondini [a,*], M. Chiappalone [b], P.D. van der Wal [a], K. Imfeld [a], N.F. de Rooij [a], M. Koudelka-Hep [a], M. Tedesco [b], S. Martinoia [b], J. van Pelt [d], G. Le Masson [c], A. Garenne [c]

[a] *Sensors, Actuators and Microsystems Laboratory, Institute of Microtechnology, University of Neuchâtel, Jaquet-Droz 1, 2007 Neuchâtel, Switzerland*
[b] *Department of Biophysical and Electronic Engineering (DIBE), University of Genova, Via Opera Pia 11a, 16145 Genova, Italy*
[c] *INSERM E358, University Bordeaux 2, 146 rue Léo Saignat, 33077 Bordeaux Cedex, France*
[d] *Netherlands Institute for Brain Research (NIBR), Meibergdreef 33, 1105 AZ Amsterdam, The Netherlands*

Abstract

Understanding how the information is coded in large neuronal networks is one of the major challenges for neuroscience. A possible approach to investigate the information processing capabilities of the neuronal ensembles is given by the use of dissociated neuronal cultures coupled to microelectrode arrays (MEAs).

Here, we describe a new strategy, based on MEAs, for studying in vitro neuronal network dynamics in interconnected sub-populations of cortical neurons. The rationale is to sub-divide the neuronal network into communicating clusters while preserving a high degree of functional connectivity within each confined sub-population, i.e. to achieve a compromise between a completely random large neuronal population and a patterned network, such as currently used with conventional MEAs.

To this end, we have realized and functionally characterized a Pt microelectrode array with an integrated EPON SU-8 clustering structure, allowing to confine five relatively large yet interconnected spontaneously developing neuronal networks (i.e. thousands of cells). The clustering structure consists of five chambers of 3 mm in diameter interconnected via 800 μm long and 300 μm wide microchannels and is integrated on the MEA of 60 thin-film Pt electrodes of 30 μm diameter. Tests of the Pt microelectrodes' stability under stimulation showed a stable behavior up to 35,000 voltage stimuli and the biocompatibility was assessed with the cultures of dissociated rat's cortical neurons achieving cultures' viability up to 60 days in vitro.

Compared to conventional MEAs, the monitoring of spontaneous and evoked activity and the computation of the Post-Stimulus Time Histogram (PSTH) within the clusters clearly demonstrates: (i) the capability to selectively activate (through poly-synaptic pathways) specific network regions and (ii) the confinement of the network dynamics mainly in the highly connected sub-networks.
© 2005 Elsevier B.V. All rights reserved.

Keywords: Microelectrode array; Clusters; SU-8 adhesion; In vitro neuronal networks; Long-term stimulation; Plasticity; Neurodynamics; Bio-MEMs

1. Introduction

The understanding of the underlying principles of the functional plasticity of the brain is a current research challenge in neurophysiology and constitutes a necessary step toward implementing these same principles in physical devices. Performing this research at the brain level introduces a very high degree of complexity due to the grand degree of connectivity. Conversely, the level of a single or a few neurons does not provide a sufficient functional connectivity. In this sense, small neuronal ensembles become an interesting intermediate level for this research and could allow acquiring a low-level, basic understanding of the network functionality.

Nowadays, nervous tissues can be cultured in vitro and kept alive for several months, while preserving their adap-

* Corresponding author. Tel.: +41 32 720 55 20; fax: +41 32 720 57 11.
E-mail address: Luca.Berdondini@unine.ch (L. Berdondini).

tive properties [1–6]. Furthermore, microelectrode arrays (MEAs), initiated by Pine [7] and Gross et al. [8], have become now a reliable interfacing technique capable of establishing a bidirectional communication between a population of connected neurons and the external world [9]. Current state of the art MEAs grant low impedance electrodes (lower than 1 MΩ at 1 kHz), a good cellular sealing [10–13] and a high charge injection capacity for an efficient stimulation [14–16].

The functional characteristics of the MEAs permit mid- to long-term recordings of both spontaneous and evoked neuronal network activity patterns and of their spatio-temporal evolution. This allows investigating learning processes and memory [17,18] and more recently also the network development [19]. However, due to the network complexity and to the fact that spontaneous activity as well as stimulations tend to exhibit complex patterns synchronized over the whole network, the identification of plasticity changes (reinforcement or inhibition) is rather difficult. In this case, it could be of fundamental importance to design neural networks at will. This complexity can be alleviated by network patterning, using adhesion promoters/inhibitors [20–27], structured PDMS layers [28,29], agar-based microchambers [30,31] and neurocages [32]. In this case, however, the random nature of

the network and its functional plasticity become relatively limited.

We have chosen a different approach to direct the organization of the neuronal network in order to facilitate the identification of interconnected pathways. This approach is based on physical barriers for clustering the network into a number of random sub-networks while preserving a high degree of functional connectivity within and among the subpopulations. The sub-networks are interconnected via integrated microchannels. An additional anticipated functionality of the clustering structure is that it might also allow localizing the stimulation in a given cluster, i.e. neuronal sub-network. In this way, a spatial segregation of network responsiveness can be promoted and functional areas can be elicited and monitored.

Among different materials that could be used for realizing the clustering structures, we have opted for EPON SU-8. This material has been used for a wide range of Bio-MEMs devices, as the insulator for a microelectrode array [33], for fabricating 3D structures in contact with neuronal cells [34] and as packaging material [35]. It shows a reduced biofouling compared to other MEMs materials and appears to be biocompatible [36]. Moreover, from the technological point of
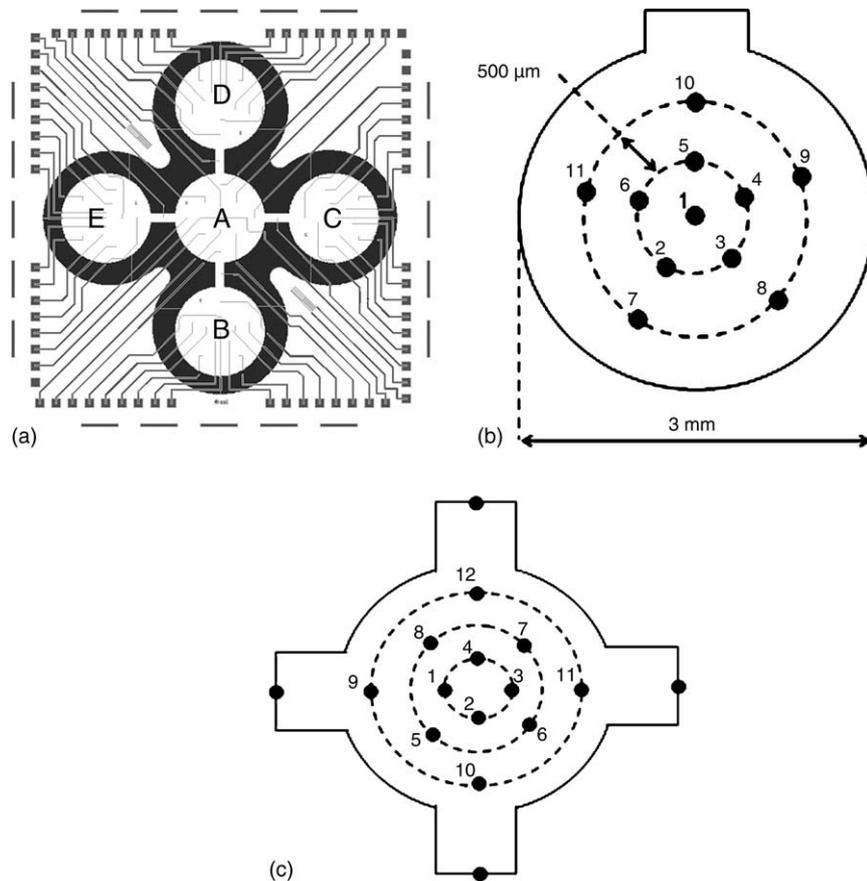

Fig. 1. Design of the microelectrodes array with the integrated clustering structures. (a) Chip layout; 60 microelectrodes are distributed in the five clusters and 1 microelectrode in each channel. Two temperature sensors (Pt-RTDs of 1 kΩ) are integrated outside the clustering structure. The overall chip dimensions are 14 mm × 14 mm. (b) Microelectrodes location in the lateral and (c) in the central clusters.

view, EPON SU-8 is a convenient material for the patterning of structures with a high aspect ratio in a single photolithographic process.

This article describes the realization and functional evaluation of a Pt-based MEA with integrated SU-8 clustering structures, so called clustered MEAs, aimed at the investigation of the functional plasticity of neuronal networks. The MEA consists of 60 thin-film Pt microelectrodes of 30 μm in diameter realized on a Pyrex substrate. The five clustering chambers interconnected via microchannels, realized in EPON SU-8, are 350 μm in height and, respectively, 3 mm in diameter and 300 μm wide. A schematic representation of the device is shown in Fig. 1a.

In the following sections, the microfabrication of the clustered MEA is described to begin with. This is followed by the evaluation of the functional lifetime of both the microelectrodes and of the clustering structures (namely the SU-8 adhesion on a Pyrex substrate). Given that the investigation of the network functional plasticity requires a long-term (up to several months) stimulation/recording of the electrophysiological activity, therefore an adequate functional lifetime of the MEAs is a prerequisite. Previous studies have shown that large amplitude biphasic potentials that are typically used in the in vitro stimulation [9,37–39] can lead to undesired electrochemical reactions, which may cause mechanical or chemical degradation of the microelectrode surface affecting the stimulation/recording capabilities and therefore the functional lifetime of the MEAs [40,41]. The results of the evaluation of the Pt microelectrodes during 35,000 stimulation cycles illustrating their good functional stability are presented. Concerning the second aspect of the functional lifetime assessment, clustering structure adhesion onto a Pyrex substrate, we show that the SU-8 adhesion can be greatly improved by using an EPON 825-based adhesion layer.

The biological functional evaluation was performed with cultures of rat's embryo cortical neurons in order to ascertain the device biocompatibility, the stimulation/recording capabilities of the microelectrodes and the functionality of the clusters for plasticity research on neuronal networks. The results demonstrate clearly such a functionality.

2. Methods

2.1. Chip design

The MEA with clustering structure (Fig. 1) was designed by using a MEMs CAD design software (Expert, Silvaco). The MEA provides a total of 60 microelectrodes with a diameter of 30 μm distributed as follows: 11 microelectrodes per lateral cluster, 1 microelectrode per open-channel and 12 microelectrodes in the central cluster. The microelectrodes are numbered and the clusters are identified by a letter (from A to E).

The clustering structures define five clustering chambers of 3 mm in diameter, connected by open-channels of 500 μm

or 800 μm in length and 300 μm in width. Additionally, for a future integration within a micro-incubation chamber, two platinum resistive temperature devices (Pt-RTDs) are integrated on chip outside the clustering structure. These sensors are designed at 1 kΩ with a serpentine structure of 10 μm in width and a total length of 10 mm.

The overall chip dimensions are 14 mm × 14 mm and fit into a glass reservoir of 2 cm of internal diameter.

2.2. Chip fabrication

The thin-film process requires three mask layers to pattern: (i) the metallic layer for the microelectrodes, the connecting leads, the bonding pads and the temperature sensors, (ii) the insulation layer to define the electrodes and contact pads and (iii) the SU-8 clustering structures. The fabrication process is summarized in Fig. 2. The 4 in. diameter substrates (Pyrex 7740 wafers, 500 μm thick from Sensor Prep Services, Elburn) were initially cleaned by successive immersions in fuming HNO_3, in buffered hydrofluoric acid (BHF) and rinsed in deionized water. The metal layers were patterned by a lift-off process by using a two layer pho-
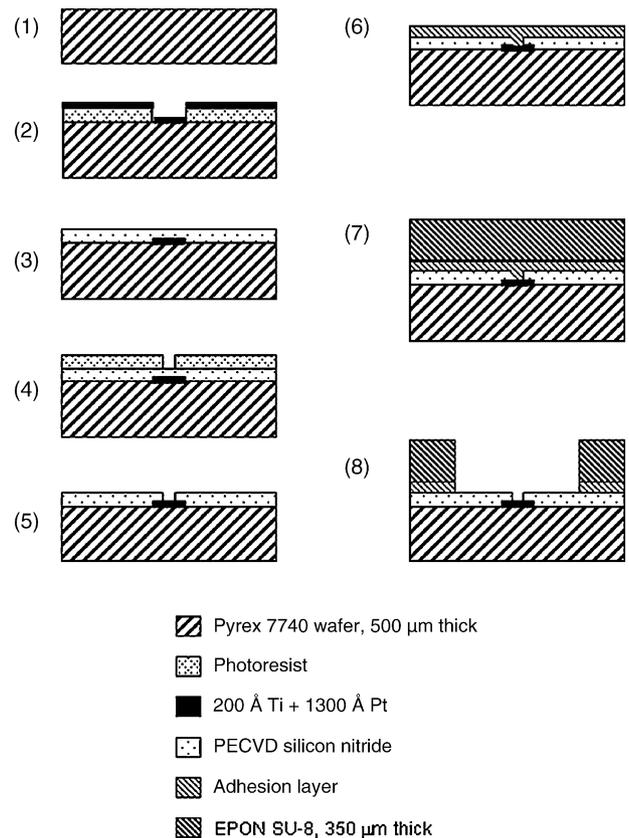

Fig. 2. Cross-section view of the microfabrication process. (1) Cleaning of the Pyrex 7740 wafer, (2) patterning of the metal layer by lift-off, (3) deposition of the silicon nitride insulation layer by PECVD, (4 and 5) photolithography and opening by SF_6/O_2 plasma etching of the microelectrode and contact pad areas, (6) silanization and spin-coating of the SU-8 adhesion layer, (7 and 8) spin-coating and patterning of the 350 μm thick layer of SU-8.

toresist technology. It consists in spin-coating the first photoresist layer (LOR3B from MicroChem Corp., USA) and a thermal treatment at 170 °C for 10 min. Then, a second positive photoresist (AZ1813 from Shipley) is spin-coated and pre-baked at 110 °C for 1 min. The wafers were then exposed in a vacuum-contact mode (mask aligner Ma-6, Karl-Süss) at 365 nm (45 mJ/cm^2) and, without a post-bake, the exposed layer developed in a 1:4 aqueous solution of AZ400K (Hoechst). This results in a photoresist structure with the second layer acting as an integrated mask for the metal evaporation. Then, a layer of 200 Å of titanium was deposited by evaporation as an adhesion layer for a 1300 Å layer of platinum. The lift-off process was performed in a solution of Remover PG (MicroChem) at 60 °C for 1 h.

The insulation layer (4000 Å thick silicon nitride) was deposited by plasma enhanced chemical vapor deposition (PECVD) and the microelectrodes and bonding pads were opened by a second photolithography followed by SF$_6$/O$_2$ plasma etching. The photoresist (AZ1518, Shipley) was stripped in acetone and the wafer rinsed with isopropanol. Finally, the wafer was cleaned in a piranha solution (5 min in concentrated H$_2$SO$_4$ and 5 min after adding a drop of H$_2$O$_2$).

The wafers were then processed with a photostructurable epoxy, the EPON SU-8 100 (MicroChem) to define the 350 μm high clustering structures. Prior to the spin-coating of SU-8, the wafers were: (i) silanized in a 10% solution of 3-glycidoxypropyltrimethoxysilane in toluene with 0.5% of water, rinsed with isopropanol and dried with nitrogen and (ii) spin-coated with an adhesion layer based on EPON 825. Following a large series of tests for optimizing the adhesion layer, the best results so far were obtained by mixing 1 g of EPON 825, 100 mg of photo-acid-generator (triarylsulfonium hexafluoroantimonate salt, Aldrich), 10 mg of silanizing agent (3-glycidoxypropyltrimethoxysilane, Aldrich) and 1 ml of the solvent γ-butyrolactone (Aldrich). Next, SU-8 100 was spin-coated, pre-baked on a hot-plate (ramp temperature from 35 to 95 °C and total time 105 min) and exposed (wavelength 365 nm and dose 1800 mJ/cm^2) using a mask aligner (AL-6, Electronic Vision) in proximity mode (separation of 50 μm). Following a post-bake (65 °C for 10 min and 95 °C for 15 min), the SU-8 was developed in PGMEA (15 min) and rinsed in isopropanol and deionized water. The adhesion layer was developed during the development of the SU-8.

Finally, the wafers were diced and the chips were cleaned in deionized water and oxygen plasma (at room temperature for 20 min) in order to remove all remaining traces of solvents and non-reticulated polymers.

2.3. Chip packaging

The chips were mounted on printed circuit boards (Micro PCB AG, Thundorf, Switzerland) that has a 12 mm in diameter aperture in the centre to provide backside light access for culture imaging with an inverted microscope, wire-bonded and the wires insulated with an epoxy resin. The PCB has dimensions of 49 mm × 49 mm and its design is compatible with the commercially available Multichannel pre-amplifier. It is realized on a standard epoxy substrate (FR-4) with a single metal layer (copper 18 μm thick) insulated with Taiyo PSR-4000.

After the chip mounting, a culture chamber of 2 cm internal diameter was glued onto the PCB. The areas of the PCB inside the glass chamber were additionally covered by a thick layer of PDMS (Sylgard 185, Dow Corning) in order to avoid any potential toxic effects that might arise from the insulation layer of the PCB. The PDMS was prepared by mixing 1 part of catalyst with 10 parts of Sylgard and polymerized at 120 °C for 1 h. This thermal treatment has the additional benefit of acting as a hard-baking step for the SU-8 layer.

2.4. Set-up for evaluating the microelectrode stability under stimulation

A waveform generator (Hewlett-Packard, HP33120A) to apply a biphasic rectangular pulse with an amplitude of 1.5 V$_{p–p}$, a period of 500 μs and a duty cycle of 50% was used. To accelerate the tests, the voltage stimuli were applied each 2 s. The microelectrodes were connected to a sensing resistor (R_{sens}) and to a digital oscilloscope (Tektronix TDS360). The sensing resistor was used to convert the current signal passing through the microelectrode–electrolyte interface in a voltage signal. Ideally, using a sensing resistor (shunt amperometer), R_{sens} should value 0 Ω, but in this case an amplifier would be needed. In order to keep the set-up simple, a higher value resistor, which has been defined empirically after measuring the applied voltage ($U_{applied}$) with respect to the stimulation voltage (U_{stim}) for different resistors and minimizing the error between them was used. It has been found that with $R_{sens} = 3.3$ kΩ the applied voltage practically fitted the ideal biphasic pulse of the waveform generator.

The experiments were performed in a physiological solution (Neurobasal Medium without L-glutamine and without phenol red from GIBCO) allowing to neglect the Ohmic drop in the solution.

The measuring system was automated by using LabView 6 (from National Instruments) and the GPIB instruments interface. In addition to the measurement of the transient current, $i(t)$, the long-term stability of the injection current versus the number of applied stimuli was also evaluated and expressed as the root-mean-square (rms) value of the injection current (computed in Matlab environment from the measured transient current acquired each 10 stimuli).

2.5. Cortical neuronal cultures

Dissociated neuronal cultures were obtained from cerebral cortices of embryonic rats at gestational day 18 (E18). The cerebral cortices of four to five rat embryos were chopped into small pieces, dissociated by enzymatic digestion in trypsin 0.125% – 20 min at 37 °C – and finally triturated with a fire-polished Pasteur pipette. Dissociated neurons were plated onto poly-D-lysine and laminin coated MEAs, in a

100 (l drop covering the electrode region ($\approx$1200 cells/mm^2); 1 h later, when cells adhered to the substrate, 1 ml of medium was added. The cells were incubated with 1% penicillin/streptomycin, 1% glutamax, 2% B-27 supplemented Neurobasal Medium (Invitrogen), in a humidified atmosphere 5% CO_2, 95% air at 37 °C [42]. Fifty percent of the medium was changed twice a week.

2.6. Electrophysiological experimental set-up

The experimental set-up is based on the MEA 60 System (Multichannel System, MCS, Reutlingen, Germany), consisting of a mounting support with integrated 60 channels pre- and filter amplifier (gain 1200$\times$), a personal computer equipped with a PCI data acquisition board for real-time signal monitoring and recording, an inverted optical microscope, an anti-vibration table and a Faraday cage. The culture chamber was sealed using silicone rings and a perfusion system as well as a temperature control were installed allowing long-time experiments. Signals were recorded and monitored by using an in-house developed software for real-time spike detection and a commercial software, MCRack (MCS) for on-line visualizations and raw data storage. Commercially available MEAs (MEA 200/30, MCS) were used for validation and comparison.

2.7. Data analysis

The typical observed electrophysiological activity in networks of dissociated neurons usually ranges from stochastic spiking to organized population bursting. A population burst consists of episodes of activity (i.e. densely packed spikes) occurring at many channels and spread over the entire network. These packages generally last from hundreds of milliseconds up to seconds and are time divided by long "silent" phases. To investigate the network behavior in spontaneous (i.e. not stimulated) conditions, we used algorithms for spike and burst detection. The spike detection algorithm consists in a hard-threshold crossing, computed using five times the standard deviation of the raw signal. The bursts were defined as sequences of three spikes occurring in less than 100 ms. A visual control of the automatic detection results corroborates the reliability of these methods (see Section 3).

To evaluate the responsiveness of the network to electrical stimulation, we computed the Post-Stimulus Time Histogram (PSTH), which represents the probability to evoke a response upon a stimulus delivered from specific site [43].

3. Results and discussion

3.1. Pt-MEA with thick SU-8 clustering structure and Pt-RTDs

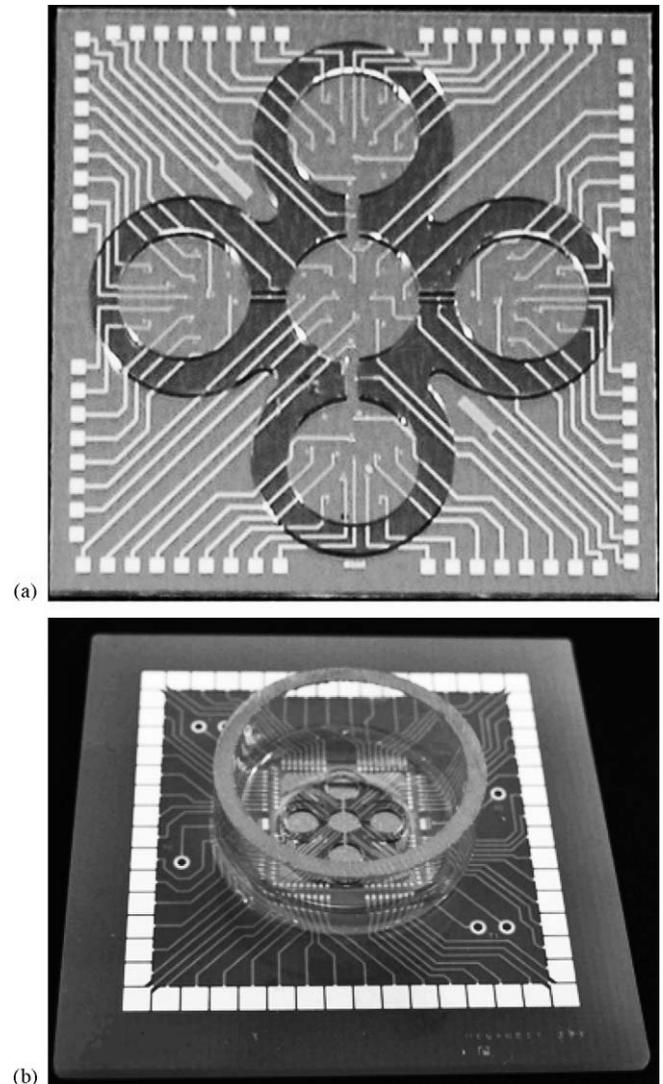The clustered MEA and a ready-to-use device are shown in Fig. 3. A fabrication yield of 85% was achieved and was

Fig. 3. (a) Optical views of a single chip (14 mm $\times$ 14 mm) and (b) of the packaged device (50 mm $\times$ 50 mm).

mainly limited by defects introduced during opening the silicon nitride passivation layer. This technological problem is often associated with large chip areas. On the other hand, the use of the two photoresist layers lift-off technique allowed achieving an excellent reproducibility and well-defined metal structure contours. Residues of SU-8, observed occasionally on the electrodes after the SU-8 development, could be efficiently removed by introducing the oxygen plasma cleaning step. Finally, the average thickness of the SU-8 structures of $346 \pm 8\,\mu$m, with a typical error in dimensions referred to the designed one, lower than 3% confirms a good fabrication process control.

The first clustering structures were realized without an adhesion layer for the SU-8. It was found that albeit the SU-8 adhesion was good and passed the scotch test after processing, the structures lifted-off after 2–3 days in physiological solution. As observed also by Voskerician et al. [36], the loss of adhesion started from the sides of the structures. This
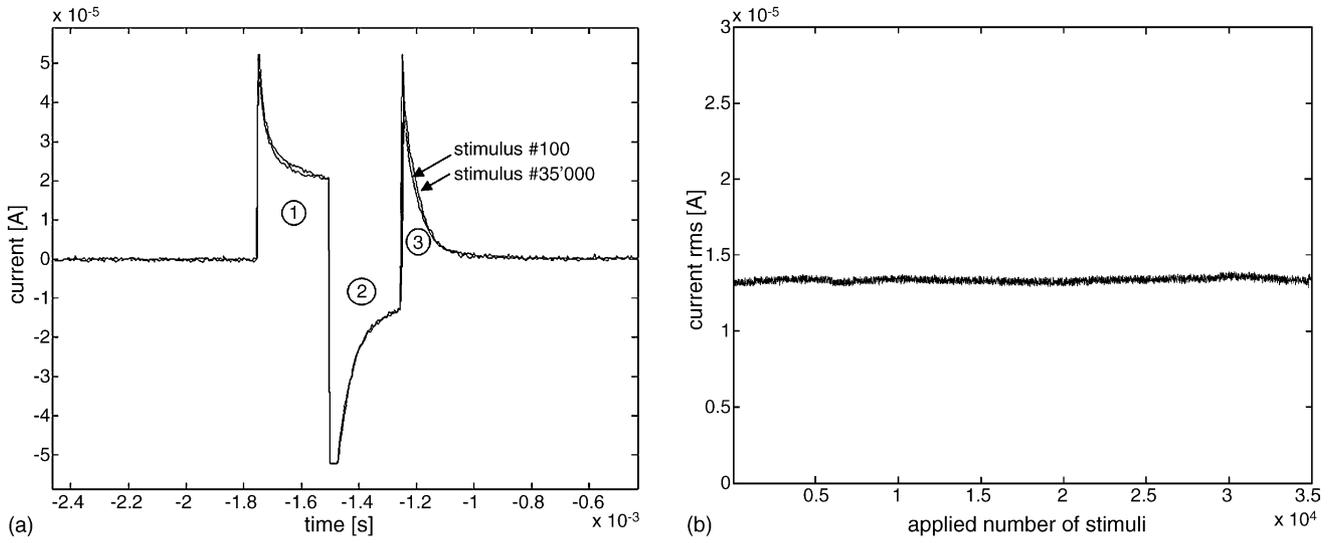
Fig. 4. (a) Measured injection current on one microelectrode, 30 μm in diameter, upon 100 and 35,000 voltage stimulations of 1.5 $V_{p–p}$ and 500 μs in period. (b) Calculated injected rms current during a stimuli versus the number of applied stimuli on one microelectrode.
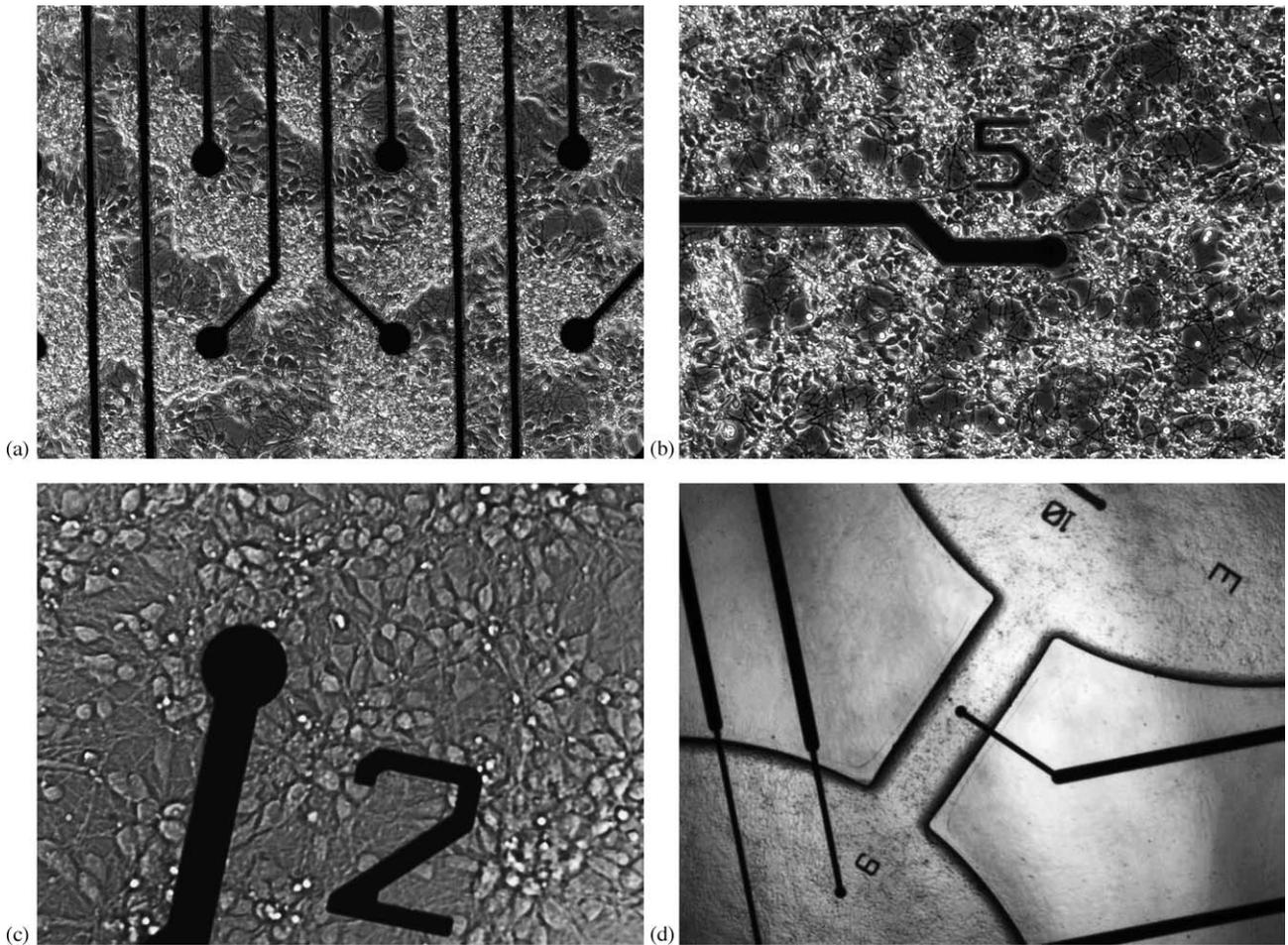

Fig. 5. Pictures of in vitro E18 cortical neurons. (a) On a conventional MEA, at 2 div and (b–d) on the clustered MEA: (b) at 2 div, (c) at 11 div and (d) at 11 div. The metal at the microelectrode sites is 40 μm in diameter.
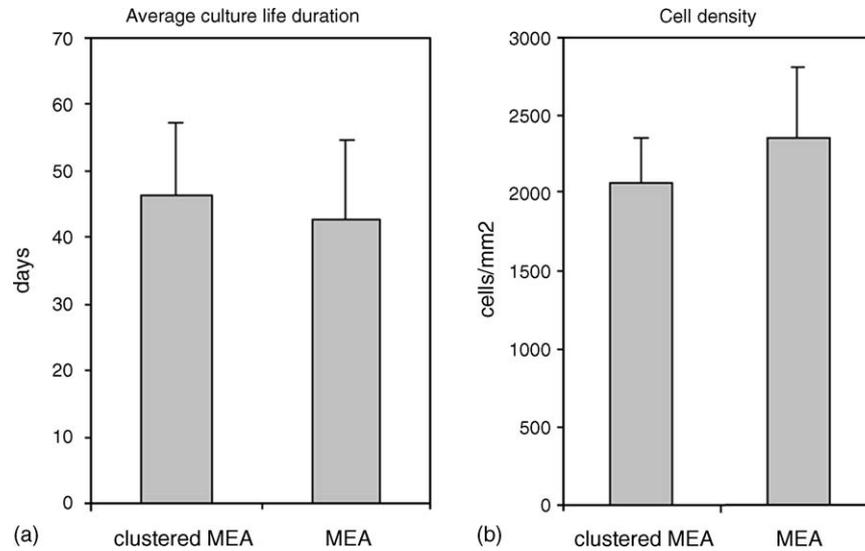
Fig. 6. Two culture health indicators on conventional and clustered MEAs. (a) Average cell culture life duration computed on the five best results from two batches. (b) Mean cell densities computed on 10 2-div samples.
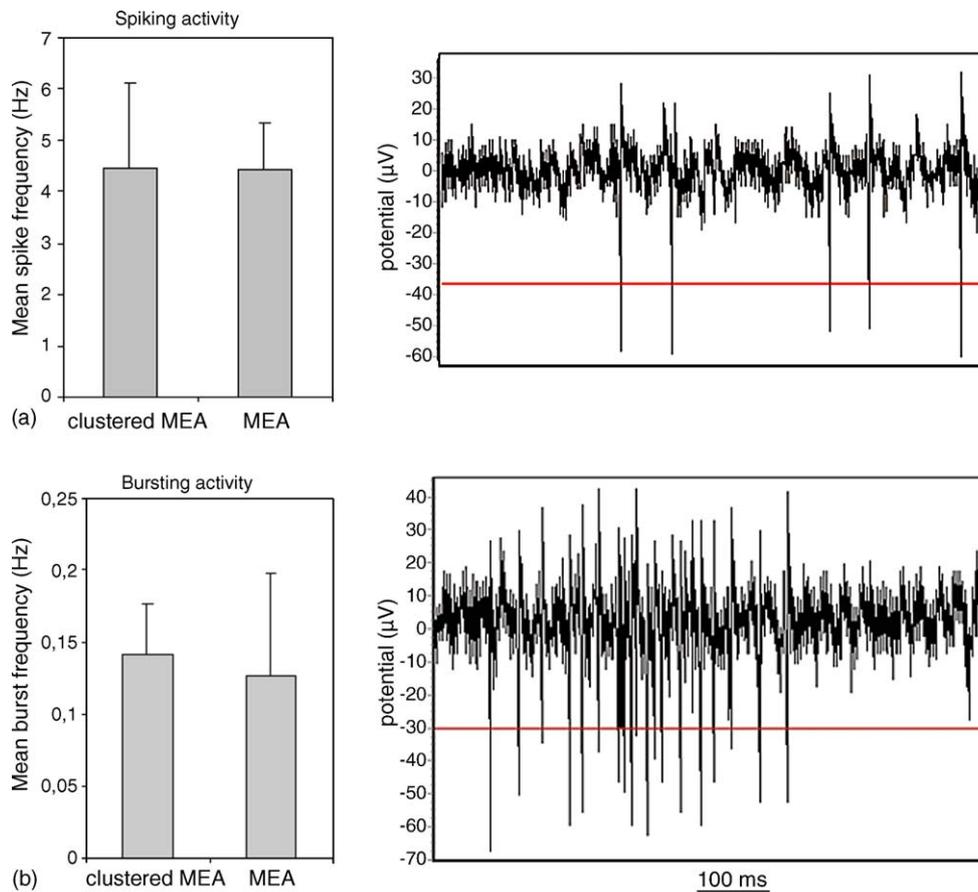

Fig. 7. Effect of the clustered organization on the mean spiking (a) and bursting (b) spontaneous activities; computed using active channel recordings of, respectively, 8 clustered MEA and 10 conventional MEA batches of 21–34 div. The corresponding recorded raw signals are shown on the right and the line stands for the detection threshold.
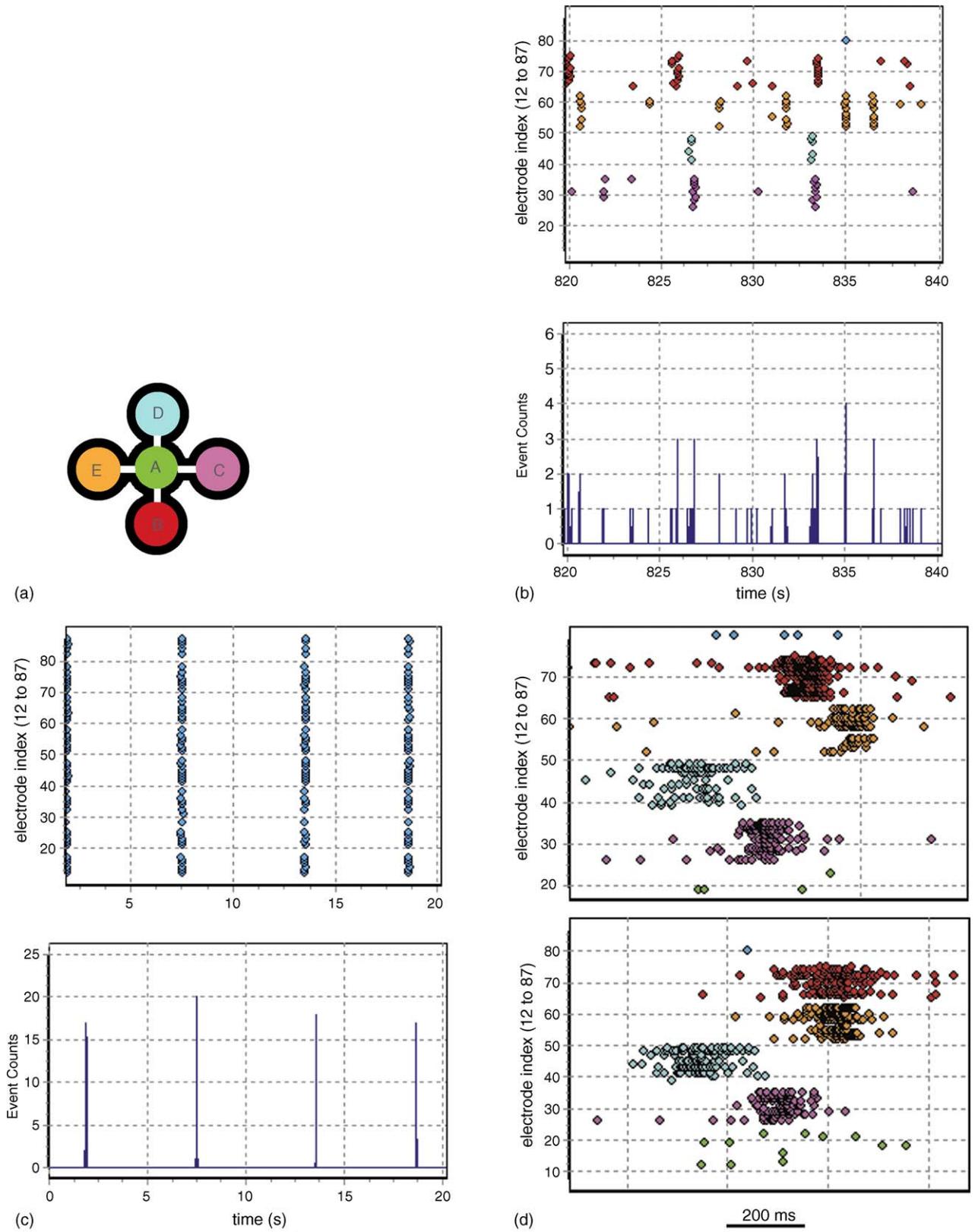
Fig. 8. Spontaneous bursting activity raster plot recorded on 21–30 div cultures for 60 s on the (a and b) clustered and (c) conventional MEAs. Raster plot spots are sorted by clusters on the clustered MEA and the burst summation is shown in the lower part. (d) Close-ups of the bursting activity on the clustered MEA showing consistent time lags.

result motivated the development of an adhesion layer able to establish a chemical bonding between the silicon nitride and the SU-8. Devices fabricated with the adhesion layer based on the EPON 825 allowed to achieve good SU-8 adhesion onto Pyrex substrates in physiological solution up to several months.

The Pt-RTD temperature sensors, although not used in this work, were characterized by measuring their resistivity at 22.4 °C before and after the PECVD silicon nitride deposition and patterning. A homogenous decrease of the resistivity of 15% was measured for a total metal thickness of 1495 Å. This resulted in an average resistivity (five points per wafer; 10 wafers measured), $\rho_{Ti–Pt}$, of 1.87×10^{-7} Ωm and in an average resistance of the Pt-RTDs of 1.0534 k$\Omega \pm 38$ Ω at 22.4 °C. The measured temperature coefficient of resistance (TCR), α, was $2.8364 \pm 0.16 \times 10^{-3}$ C^{-1}.

3.2. Microelectrode evaluation under long-term stimulation

As already emphasized, the microelectrode functional stability under long-term voltage stimulation is of crucial importance for studying plasticity in neuronal networks. Fig. 4a shows a typical example of the recorded injection currents after 100 and 35,000 biphasic voltage stimuli with the amplitude and duty cycle corresponding to the neuronal stimulation protocol used subsequently. The three phases of the stimulus train correspond, respectively, to the anodic (1) and cathodic (2) pulses followed by a discharge (3). The practically superposed responses after 100 and 35,000 stimuli demonstrate an adequate stimulation functionality of the Pt microelectrodes.

The stability of the charge injection is more evident upon computing the root-mean-square of the injection current with respect to the number of delivered stimuli (Fig. 4b). It can be seen that Pt microelectrodes show a stable injection root-mean-square current of 13.3 ± 0.35 μA per microelectrode (rms current density 1.88 A/cm^2) over 35,000 stimuli of 1.5 V$_{p–p}$.

The average injected charge densities over 35,000 stimuli for each phase of the stimulus train (1–3) are, respectively, $Q_1 = 4.62 \times 10^{-4}$ C/cm^2, $Q_2 = -4.53 \times 10^{-4}$ C/cm^2 and $Q_3 = -1.47 \times 10^{-4}$ C/cm^2. A dissymmetry between the positive and negative phase is observed in terms of the injected charge (0.9×10^{-5} C/cm^2) and is not, as might be expected for a 50% duty cycle high-amplitude voltage stimuli, compensated for in the discharge phase [44–46]. However, the stability of the injection current demonstrates that this does not affect the electrodes' functional reliability. This has been further confirmed by cyclic voltammetry, where practically unchanged voltammograms were obtained prior to and after the functional stability experiments (results not shown). Moreover, the charge injection dissymmetry does not seem to induce any problems in the electrophysiological recordings (see below).

3.3. Functional experiments with rat's cortical neuronal cultures

The effects of the clustering structure on the spontaneous and evoked network activities were evaluated by comparing the recordings on clustered and conventional MEAs. Neuronal cultures on the clustered MEAs were routinely kept active and healthy up to 45–60 days (Figs. 5 and 6). Furthermore, the distributed organization was fully compatible with long-term cell cultures and comparable to that observed on conventional MEAs.

Comparing the spontaneous spiking and bursting activity rates recorded on, respectively, conventional and clustered MEAs, as shown in Fig. 7, no apparent difference of the mean level of activity was observed. However, a
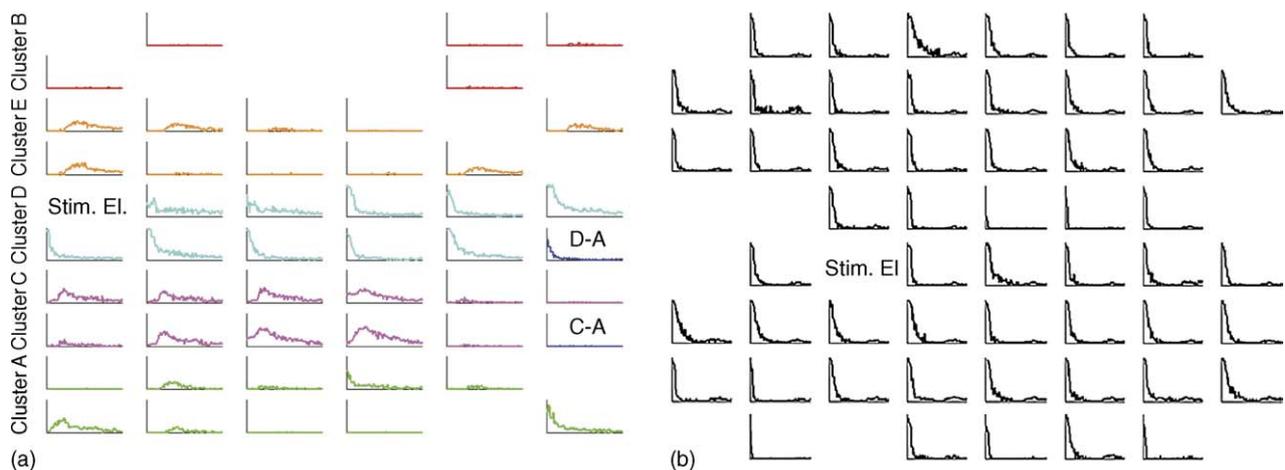

Fig. 9. Post-Stimulus Time Histogram (PSTH) on (a) a clustered MEA and (b) a conventional MEA. (a) The graph reports a 10×6 grid where each cell represents the PSTH computed for the recording microelectrodes, belonging to different clusters as indicated by the five labels. Electrodes in the channels are indicated by the letters of the connected clusters. Note how the clustered MEA is able to evoke responses of different shapes and features according to the belonging clusters. Cluster B is not active. (b) The graph reports a 8×8 grid, built according to the conventional MEA layout. Note that within the entire array it is not possible to distinguish different features of the PSTH. The X-axis scale is [0, 400] ms, while the Y-axis scale is [0, 1].

more detailed examination of the bursting activity patterns between and within the clusters revealed certain differences. In comparison with conventional MEA, where cultures tend rapidly toward a synchronized bursting activity distributed over the entire microelectrode array, on the clustered MEAs the recordings exhibited a distribution of synchronous bursts in the clusters and asynchronous bursts between the clusters (Fig. 8b and c). This is even more evident when all the burst occurrences from all the microelectrodes are considered (Fig. 8b and c, lower part). The asynchronous bursting between the clusters resulted in a sequential pattern of bursts with consistent time lags (Fig. 8d) and was routinely found from one culture to another. Thus, asynchronous bursting areas might be linked to the distributed organization of the culture.

The behavior of the network in interconnected sub-populations was even more evident looking at the evoked activity patterns. The network responsiveness to localized stimulations was evaluated by means of the Post-Stimulus Time Histogram as shown in Fig. 9. It can be seen that the clustered MEA imparts a distinct variability on the network responses to a single stimulation (i.e. a train of 50 pulses at 0.2 Hz and 1.5 V_{p-p} from a single electrode): the PSTH shape was different for separated clusters, while it maintained the same features within the same cluster. The sub-population in the stimulated cluster (cluster D in Fig. 9a) shows a higher probability of evoked response, yet the evoked activity clearly propagates to the connected clusters. This variability of the network responsiveness is not observed on a conventional MEA (Fig. 9b), where the network freely grows in the avail-
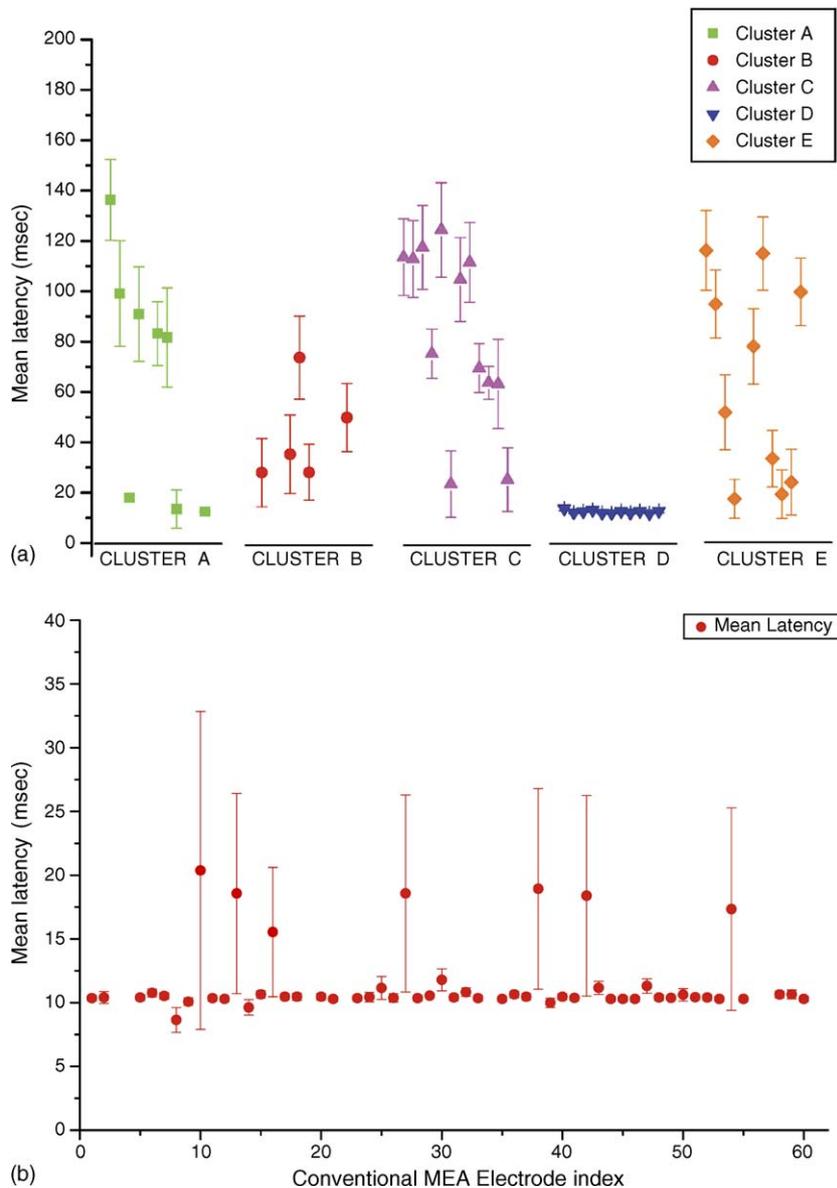

Fig. 10. Mean latency of the evoked responses computed from data of Fig. 9 on (a) a clustered MEA and (b) a conventional MEA.

able space, producing a dense layer of strongly connected cells. Upon stimulation in this condition, each site of the array shows a very similar response.

Fig. 10 presents the computed mean latency of the responses to the delivered stimuli. Compared to the stimulated cluster, the other clusters show a longer latency and a larger variability in the response time, demonstrating the sub-populations interconnections and the different pathways involved in the network dynamics. It is worthwhile to note that a very similar behavior is observed between the network in the stimulated cluster and the whole network on a conventional MEA.

4. Conclusions

In this paper, the fabrication, the functional evaluation and the biological validation of a microelectrode array with an integrated SU-8 clustering structure were described. The purpose of the interconnected cluster structure is to reduce the isotropic network distribution, as well as to discern local relations between cell growth, activity and their involvement according to their use as input, output or processing areas.

The recording of the spontaneous activity demonstrated a clear difference in the distribution of the bursting activity between the conventional and clustered MEAs. Thus, this approach does not prevent local bursting activity (in the sub-population) but allows its distribution over the clusters. The cluster functionality of confining the network dynamics mainly in the sub-networks was further confirmed by recording the network evoked activity. The computed PSTHs clearly show the localization of the stimulation in the cluster to which the stimulating electrode belongs, yet the evoked signal propagates through the connecting channels, influencing the activity of the other sub-populations. The shape of the PSTH does not change within the cluster from which the stimulus is delivered, while clear delays and differences in the number of evoked spikes are visible in the others. The stimulated cluster response was very similar to the one recorded on a conventional MEA confirming the network organization in interconnected sub-populations.

An organization of neuronal networks in interconnected sub-populations is an important step further on in the investigation of the functional and anatomical aspects of distributed learning processes. The proof of concept of the clustering structure functionality opens new prospects for investigating in vitro interactions among large assemblies of neurons or co-cultured populations (e.g., neocortex and hippocampus) as well as the basic learning mechanisms and network plasticity.

Acknowledgments

References

[1] S. Marom, D. Eytan, Learning in ex-vivo developing networks of cortical neurons, in: J. van Pelt, al. et (Eds.), Progress in Brain Research, vol. 147, Elsevier Science Ltd., 2004, pp. 189–199 (Chapter 14).

[2] G. Shahaf, S. Marom, Learning in networks of cortical neurons, J. Neurosci. 21 (22) (2001) 8782–8788.

[3] K. Ganguly, M.-M. Poo, L. Kiss, Enhancement of presynaptic neuronal excitability by correlated presynaptic and postsynaptic spiking, Nat. Neurosci. 3 (10) (2000) 1018–1026.

[4] H.-Z.W. Tao, L.I. Zhang, G.-Q. Bi, M.-M. Poo, Selective presynaptic propagation of long-term potentiation in defined neural networks, J. Neurosci. 20 (9) (2000) 3233–3243.

[5] G.-Q. Bi, M.-M. Poo, Distributed synaptic modification in neural networks induced by patterned stimulation, Nature 401 (6755) (1999) 792–796.

[6] Y. Jimbo, Recording neural activity by electrode-array substrates, Electrochemistry 67 (3) (1999) 276–279.

[7] J. Pine, Recording action potentials from cultured neurons with extracellular micro-circuit electrodes, J. Neurosci. Methods 2 (1) (1980) 19–31.

[8] G.W. Gross, A.N. Williams, J.H. Lucas, Recording of spontaneous activity with photoetched microelectrode surfaces from mouse spinal neurons in culture, J. Neurosci. Methods 5 (1–2) (1982) 13–22.

[9] S. Potter, Distributed processing in cultured neuronal networks, in: M.A.L. Nicolelis (Ed.), Progress in Brain Research, vol. 130, Elsevier Science Ltd., 2001, pp. 49–62 (Chapter 4).

[10] W. Rutten, J.M. Mouveroux, J. Buitenweg, C. Heida, T. Ruardij, E. Marani, E. Lakke, Neuroelectronic interfacing with cultured multielectrode arrays toward a cultured probe, in: Proceedings of the IEEE, July 2001.

[11] V. Kiessling, P. Fromherz, B. Muller, Extracellular resistance in cell adhesion measured with a transistor probe, Langmuir 16 (7) (2000) 3517–3521.

[12] M.P. Maher, J. Pine, J. Wright, Y.-C. Tai, The Neurochip: a new multielectrode device for stimulating and recording from cultured neurons, J. Neurosci. Methods 87 (1) (1999) 45–56.

[13] W.G. Regehr, J. Pine, C.S. Cohan, M.D. Mischke, D.W. Tank, Sealing cultured invertebrate neurons to embedded dish electrodes facilitates long-term stimulation and recording, J. Neurosci. Methods 30 (2) (1989) 91–106.

[14] T. Nyberg, O. Inganas, H. Jerregard, Polymer hydrogel microelectrodes for neural communication, Biomed. Microdevices 4 (1) (2002) 43–52.

[15] J.D. Weiland, D.J. Anderson, M.S. Humayun, In vitro electrical properties for iridium oxide versus titanium nitride stimulating electrodes, IEEE Trans. Biomed. Eng. 49 (12) (2002) 1574–1579.

[16] A. Blau, C. Ziegler, M. Heyer, F. Endrest, G. Schwitzgebel, T. Matthies, T. Stieglitz, J.-U. Meyer, W. Göpel, Characterization and optimization of microelectrode arrays for in vivo nerve signal recording and stimulation, Biosens. Bioelectron. 12 (9–10) (1997) 883–892.

[17] Y. Jimbo, T. Tateno, H.P.C. Robinson, Simultaneous induction of pathway-specific potentiation and depression in networks of cortical neurons, Biophys. J. 76 (2) (1999) 670–678.

[18] T.B. DeMarse, D.A. Wagenaar, A.W. Blau, S.M. Potter, The neurally controlled animat: biological brains acting with simulated bodies, Auton. Robot. 11 (3) (2001) 305–310.

[19] J. Van Pelt, P.S. Wolters, M.A. Corner, G.J.A. Ramakers, W.L.C. Rutten, J. Van Pelt, Long-term characterization of firing dynamics of spontaneous bursts in cultured neural networks, IEEE Trans. Biomed. Eng. 51 (11) (2004) 2051–2062.

[20] H. Moriguchi, K. Takahashi, Y. Sugio, Y. Wakamoto, I. Inoue, Y. Jimbo, K. Yasuda, On-chip neural cell cultivation using agarose-microchamber array constructed by a photothermal etching method, Electr. Eng. Jpn. 146 (2) (2004) 37–42.

[21] A.K. Vogt, L. Lauer, W. Knoll, A. Offenhausser, Micropatterned substrates for the growth of functional neuronal networks of defined geometry, Biotechnol. Prog. 19 (5) (2003) 1562–1568.

[22] C.K. Yeung, L. Lauer, A. Offenhäusser, W. Knoll, Modulation of the growth and guidance of rat brain stem neurons using patterned extracellular matrix proteins, Neurosci. Lett. 301 (2001) 147–150.

[23] P. Heiduschka, I. Romann, H. Ecken, M. Schoning, W. Schuhmann, S. Thanos, Defined adhesion and growth of neurones on artificial structured substrates, Electrochim. Acta 47 (1–2) (2001) 299–307.

[24] M. Scholl, C. Sprossler, M. Denyer, M. Krause, K. Nakajima, A. Maelicke, W. Knoll, A. Offenhausser, Ordered networks of rat hippocampal neurons attached to silicon oxide surfaces, J. Neurosci. Methods 104 (1) (2000) 65–75.

[25] C.L. Klein, M. Scholl, A. Maelicke, Neuronal networks in vitro: formation and organization on biofunctionalized surfaces, J. Mater. Sci.: Mater. Med. 10 (12) (1999) 721–727.

[26] S. Saneinejad, M.S. Shoichet, Patterned glass surfaces direct cell adhesion and process outgrowth of primary neurons of the central nervous system, J. Biomed. Mater. Res. 42 (1) (1998) 13–19.

[27] C. Wyart, C. Ybert, L. Bourdieu, C. Herr, C. Prinz, D. Chatenay, Constrained synaptic connectivity in functional mammalian neuronal networks grown on patterned surfaces, J. Neurosci. Methods 117 (2) (2002) 123–131.

[28] L. Griscom, P. Degenaar, B. LePioufle, E. Tamiya, H. Fujita, Techniques for patterning and guidance of primary culture neurons on micro-electrode arrays, Sens. Actuators B, Chem. 83 (1–3) (2002) 15–21.

[29] E. Ostuni, R. Kane, G.M. Whitesides, C.S. Chen, D.E. Ingber, Patterning mammalian cells using elastomeric membranes, Langmuir 16 (20) (2000) 7811–7819.

[30] Y. Sugio, K. Komjima, H. Moriguchi, K. Takahashi, K. Yasuda, An agar-based on-chip neural-cell-cultivation system for stepwise control of network pattern generation during cultivation, Sens. Actuators B, Chem. 99 (1) (2004) 156–162.

[31] I. Suzuki, Y. Sugio, I.H. Moriguch, A. Hattori, K. Yasuda, Y. Jimbo, Pattern modification of a neuronal network for individual-cell-based electrophysiological measurement using photothermal etching of an agarose architecture with a multielectrode array, in: IEE Proceedings Nanobiotechnology, 2004.

[32] M.P. Maher, J. Pine, J. Wright, Y.-C. Tai, The Neurochip: a new multielectrode device for stimulating and recording from cultured neurons, J. Neurosci. Methods 87 (1) (1999) 45–56.

[33] M.O. Heuschkel, M. Fejtl, M. Raggenbass, D. Bertrand, P. Renaud, A three-dimensional multi-electrode array for multi-site stimulation and recording in acute brain slices, J. Neurosci. Methods 114 (2) (2002) 135–148.

[34] Y. Choi, R. Powers, A.B. Frazier, M.G. Allen, V. Vernekar, M.C. LaPlaca, High Aspect Ratio SU-8 Structures for 3-D Culturing of Neurons, American Society of Mechanical Engineers, Micro-Electromechanical Systems Division Publication (MEMS), 2003, pp. 651–654.

[35] L.A. Francis, C. Bartic, A. Campitelli, J.-M. Friedt, A SU-8 liquid cell for surface acoustic wave biosensors, in: Proceedings of SPIE—The International Society for Optical Engineering, 2004.

[36] G. Voskerician, M.S. Shive, R.S. Shawgo, H. von Recum, J.M. Anderson, M.J. Cima, R. Langer, Biocompatibility and biofouling of MEMS drug delivery devices, Biomaterials 24 (11) (2003) 1959–1967.

[37] D.A. Wagenaar, J. Pine, S.M. Potter, Effective parameters for stimulation of dissociated cultures using multi-electrode arrays, J. Neurosci. Methods 138 (1–2) (2004) 27–37.

[38] Y. Jimbo, H.P.C. Robinson, A. Kawana, Strengthening of synchronized activity by tetanic stimulation in cortical cultures: application of planar electrode, IEEE Trans. Biomed. Eng. 45 (11) (1998) 1297–1304.

[39] H. Oka, K. Shimono, R. Ogawa, H. Sugihara, M. Taketani, A new planar multielectrode array for extracellular recording: application to hippocampal acute slice, J. Neurosci. Methods 93 (1) (1999) 61–67.

[40] S. Mailley, M. Hyland, P. Mailley, J.A. McLaughlin, E.T. McAdams, Thin film platinum cuff electrodes for neurostimulation: in vitro approach of safe neurostimulation parameters, Bioelectrochemistry 63 (1–2) (2004) 359–364.

[41] A. Norlin, J. Pan, C. Leygraf, Investigation of interfacial capacitance of Pt, Ti and TiN coated electrodes by electrochemical impedance spectroscopy, Biomol. Eng. 19 (2–6) (2002) 67–71.

[42] G.J. Brewer, Isolation and culture of adult rat hippocampal neurons, J. Neurosci. Methods 71 (2) (1997) 143–155.

[43] F. Rieke, D. Warland, R. de Ruyter van Steveninck, W. Bialek, Spikes: Exploring the Neural Code, The MIT Press, Cambridge, Massachusetts, 1997.

[44] J. McHardy, L.S. Robblee, J.M. Marston, S.B. Brummer, Electrical-stimulation with Pt electrodes (4) factors influencing Pt dissolution in inorganic saline, Biomaterials 1 (3) (1980) 129–134.

[45] L.S. Robblee, J. McHardy, J.M. Marston, S.B. Brummer, Electrical-stimulation with Pt electrodes (5) the effect of protein on Pt dissolution, Biomaterials 1 (3) (1980) 135–139.

[46] S.B. Brummer, M.J. Turner, Electrical-stimulation of nervous-system-principle of safe charge injection with noble-metal electrodes, Bioelectrochem. Bioenerg. 2 (1) (1975) 13–25.